



Homogeneous antibody and CAR-T cells with improved effector functions targeting SSEA-4 glycan on pancreatic cancer

Chih-Wei Lin^{a,b,1}, Yu-Jen Wang^{b,c,1}, Ting-Yen Lai^b, Tsui-Ling Hsu^b, Shin-Ying Han^b, Han-Chung Wu^d, Chia-Ning Shen^b , Van Dang^e, Ming-Wei Chen^e, Lan-Bo Chen^{e,f}, and Chi-Huey Wong^{a,b,2}

^aDepartment of Chemistry, The Scripps Research Institute, La Jolla, CA 92037; ^bGenomics Research Center, Academia Sinica, Taipei 11529, Taiwan; ^cInstitute of Biochemical Sciences, National Taiwan University, Taipei 10617, Taiwan; ^dInstitute of Cellular and Organismic Biology, Academia Sinica, Taipei 11529, Taiwan; ^eDepartment of Cell Biology, CHO Pharma USA, Inc., Woburn, MA 01801; and ^fDepartment of Pathology, Harvard Medical School, Boston, MA 02115

Contributed by Chi-Huey Wong, October 13, 2021 (sent for review August 11, 2021; reviewed by Xi Chen and Bruce R. Zetter)

Pancreatic cancer is usually asymptomatic in the early stages; the 5-y survival rate is around 9%; and there is a lack of effective treatment. Here we show that SSEA-4 is more expressed in all pancreatic cancer cell lines examined but not detectable in normal pancreatic cells; and high expression of SSEA-4 or the key enzymes *B3GALT5* + *ST3GAL2* associated with SSEA-4 biosynthesis significantly lowers the overall survival rate. To evaluate potential new treatments for pancreatic cancer, homogeneous antibodies with a well-defined Fc glycan for optimal effector functions and CAR-T cells with scFv construct designed to target SSEA-4 were shown highly effective against pancreatic cancer in vitro and in vivo. This was further supported by the finding that a subpopulation of natural killer (NK) cells isolated by the homogeneous antibody exhibited enhancement in cancer-cell killing activity compared to the unseparated NK cells. These results indicate that targeting SSEA-4 by homologous antibodies or CAR-T strategies can effectively inhibit cancer growth, suggesting SSEA-4 as a potential immunotherapy target for treating pancreatic disease.

pancreatic cancer | SSEA-4 expression | homogeneous antibody | CAR-T

Pancreatic ductal adenocarcinoma (PDAC) is the most common type of pancreatic cancer. The lack of effective treatment (1–4) along with problems of tumor heterogeneity, complex tumor microenvironment, drug resistance, and lack of early detection (5–7) are the major challenges in development of effective treatment for PDAC. These challenges point to an urgent unmet medical need for identification of new targets for development of early diagnosis and better treatment for this disease. In addition, although a variety of cell surface markers have been explored in the past, most of these markers are also expressed in normal cells or are frequently mutated to resist treatments, making the targeted therapy strategy difficult to achieve effectively (8–11). Altered glycolipids generated by aberrant glycosylation have been recognized as potential anti-cancer targets (12, 13), especially many tumor-associated carbohydrate antigens (TACA) (13) discovered to date are highly sialylated or fucosylated and often found on the surface of cancer cells and their stem cells (14, 15). Altered glycosylation is a hallmark of tissue inflammation and neoplasia due to differential expression of glycosyltransferases. Compared to proteins, glycans are smaller in size and are synthesized by many glycan-associated enzymes; so when the glycans are assembled abnormally in diseased cells, their structures could become unique and nonself and could be used as markers with more distinct structural difference than proteins (15–18). Among the glycoconjugates of TACA, stage-specific embryonic antigen-4 (SSEA-4) is a cell-surface glycosphingolipid (GSL) used to define human embryonic stem cells (ESCs) and human embryonic carcinoma cells or induced pluripotent stem cells (iPSCs) (19, 20). SSEA-4 usually

would disappear after stem cell differentiation and reappear with the other two globo-series GSLs, SSEA-3 and Globo-H (21–24). The importance of globo-series GSLs as unique markers in cancer progression is further supported by the ongoing phase 3 global trial of a Globo-H vaccine against triple-negative breast cancer (NCT03562637). In this study, as part of our efforts to identify new targets for PDAC, we sought to investigate the role of SSEA-4 in cancer patients and found that its high expression correlated with poor survival. In addition, we also showed the development of a homogeneous antibody with improved effector functions and a CAR-T strategy to target SSEA-4 that hold a significant promise for the treatment of PDAC.

Result

Expression of SSEA-4 in Pancreatic Cancer and Normal Cells. In the biosynthesis of globo-series GSLs which are exclusively expressed on cancer cells (Fig. 1A), SSEA-3 is first generated from Gb4 by B3GALT5 and converted to SSEA-4 and Globo-H by ST3GAL2 and FUT1/FUT2, respectively. To understand the expression level of SSEA-4 in pancreatic cancer, we analyzed 14 pancreatic cancer cell lines by flow cytometry. The result (Fig. 1B and *SI Appendix, Table S1A*) showed that all of the 14 pancreatic cancer cell lines, including those with drug resistance, i.e., PANC-1, AsPC-1, MIAPaCa-2, expressed SSEA-4, whereas 7 were Globo-H positive and 4 were SSEA-3 positive, and the expression level of SSEA-4 was higher than SSEA-3 and Globo-H (Fig. 1C). In contrast, the human pancreatic epithelial normal cell line, HPEpiC, had no expression of globo-series GSLs. Besides, the level of SSEA-4 expression in HPAC (human pancreatic adenocarcinoma) cancer cell lines is higher than Globo-H as shown in the cell lines stained with specific Globo-H antibody and SSEA-

Significance

Pancreatic cancer treatments remain challenging due to late diagnosis and intrinsic resistance to conventional treatments. In this study, we demonstrate the use of the homogeneous SSEA-4 antibody and CAR-T cells for effective treatment in pancreatic cancer and suggest that targeting SSEA-4 has the potential to treat pancreatic cancer.

Author contributions: C.-W.L. and C.-H.W. designed research; C.-W.L., Y.-J.W., T.-Y.L., and S.-Y.H. performed research; H.-C.W. and C.-N.S. contributed reagents; C.-W.L. and T.-L.H. analyzed data; and C.-W.L., V.D., M.-W.C., L.-B.C., and C.-H.W. wrote the paper. Reviewers: X.C., University of California, Davis; B.R.Z., Boston Children's Hospital. The authors declare no competing interest.

Published under the [PNAS license](#).
¹C.-W.L. and Y.-J.W. contributed equally to this work.

²To whom correspondence may be addressed. Email: wong@scripps.edu.

This article contains supporting information online at <http://www.pnas.org/lookup/suppl/doi:10.1073/pnas.2114774118/-DCSupplemental>.

Published December 7, 2021.

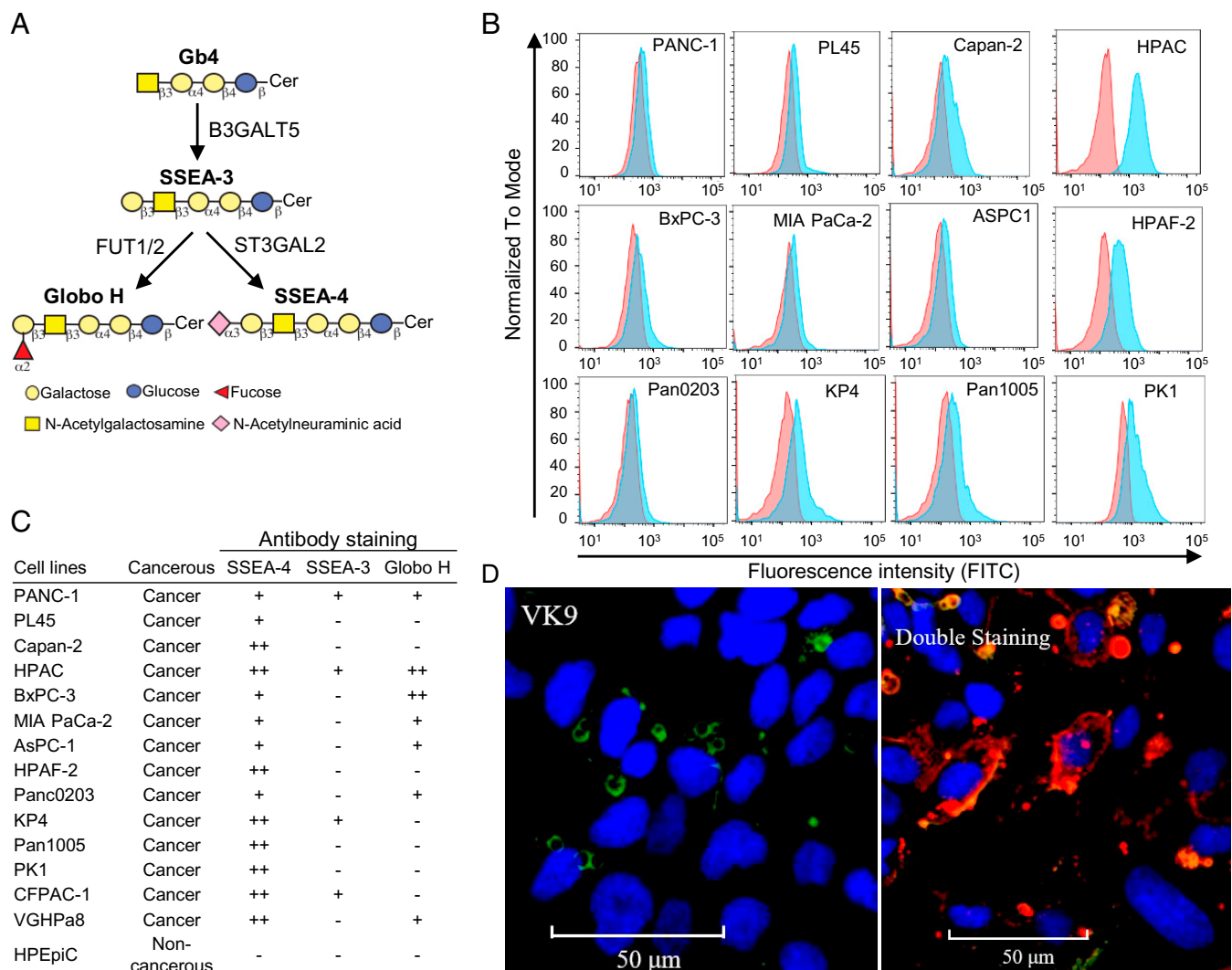


Fig. 1. Expression of SSEA-4 in pancreatic cancer and normal cells. (A) Schematic diagram of the biosynthesis of globo-series GSLs. SSEA-3 (Gb5), the precursor of SSEA-4 and Globo-H, is first synthesized from Gb4 by B3GALT5, then converted to SSEA-4 or Globo-H by ST3GAL2 or FUT1/2, respectively. (B) Flow cytometric analysis of SSEA-4 expression in pancreatic cancer cell lines. Pancreatic cancer cell lines were stained with SSEA-4 antibody (MC-813-70) conjugated with fluorescein isothiocyanate (FITC), and the staining intensity was analyzed with flow cytometry. The histograms of the cells stained with SSEA-4 antibody and isotype control are shown in blue and red, respectively. (C) The expression profiles of globo-series GSLs in pancreatic cancer and normal cell lines. Cell lines with less than 5% of total cells stained positively were labeled as “-,” with 5 to 20% as “+,” and with more than 20% as “++.” (D) Opera Phenix images of HPAC cells mixed with FITC-VK9 antibody (green) against Globo-H (Left) or with APC-MC-813-70 (red) plus FITC-VK9 antibodies (0.5 μ g/mL:25 μ g/mL, 1:50) against SSEA-4 and Globo-H, respectively (Right). Both antibodies have similar affinity to their ligands with K_d in the nanomolar range. Hoechst 33342 was used to stain the nucleus (blue). Details are described in *SI Appendix, Materials and Methods*.

4 antibody that recognize their ligands with K_d in the nanomolar range (Fig. 1D). It was also observed that SSEA-4 is more accessible to its antibody even in the presence of 50-fold excess of anti-Globo-H antibody. We also examined the presence of globo-series GSLs in other types of cancer (i.e., breast, lung, and brain). The results (*SI Appendix, Fig. S1 and Table S1B*) showed that many of these cancer cell lines expressed globo-series GSLs, and the expression level of SSEA-4 was also higher than that of the other two GSLs. All these studies further suggest that globo-series GSLs are cancer specific and among them SSEA-4 is a better target for antibody therapy.

Since SSEA-4 is highly expressed on pancreatic cancer cells, its expression profile and role in pancreatic cancer are further investigated. We first analyzed the mRNA levels of *B3GALT5*, *ST3GAL2*, *FUT1*, and *FUT2* associated with the biosynthesis of globo-series GSLs in cancer patients and normal samples using gene expression profiling interactive analysis (GEPIA) with

collected RNA sequencing (RNA-seq) data of patients. The expression profiles of *B3GALT5*, *ST3GAL2*, *FUT1*, and *FUT2* across all tumor samples and paired normal tissues are shown in Fig. 2A. The level of *B3GALT5* mRNA is significantly higher in pancreatic adenocarcinoma (PAAD) than in the corresponding normal tissues. This result suggests that *B3GALT5*, the key enzyme associated with the biosynthesis of globo-series GSLs, is more expressed in PAAD than in other cancer cell types, consistent with our previous finding that knockdown of *B3GALT5* led to breast cancer cell apoptosis, while there was no effect on normal cells (22). In addition, *ST3GAL2* and *FUT2* are more expressed in PAAD than in the corresponding normal tissues (Fig. 2B). We then investigated the mRNA expression levels of *B3GALT5* and *ST3GAL2* using the clinical Kaplan–Meier (KM)-plotter database. Kaplan–Meier analysis of PAAD patients with high expression of *B3GALT5* showed significantly lower overall survival (OS) than those with low expression (hazard ratio

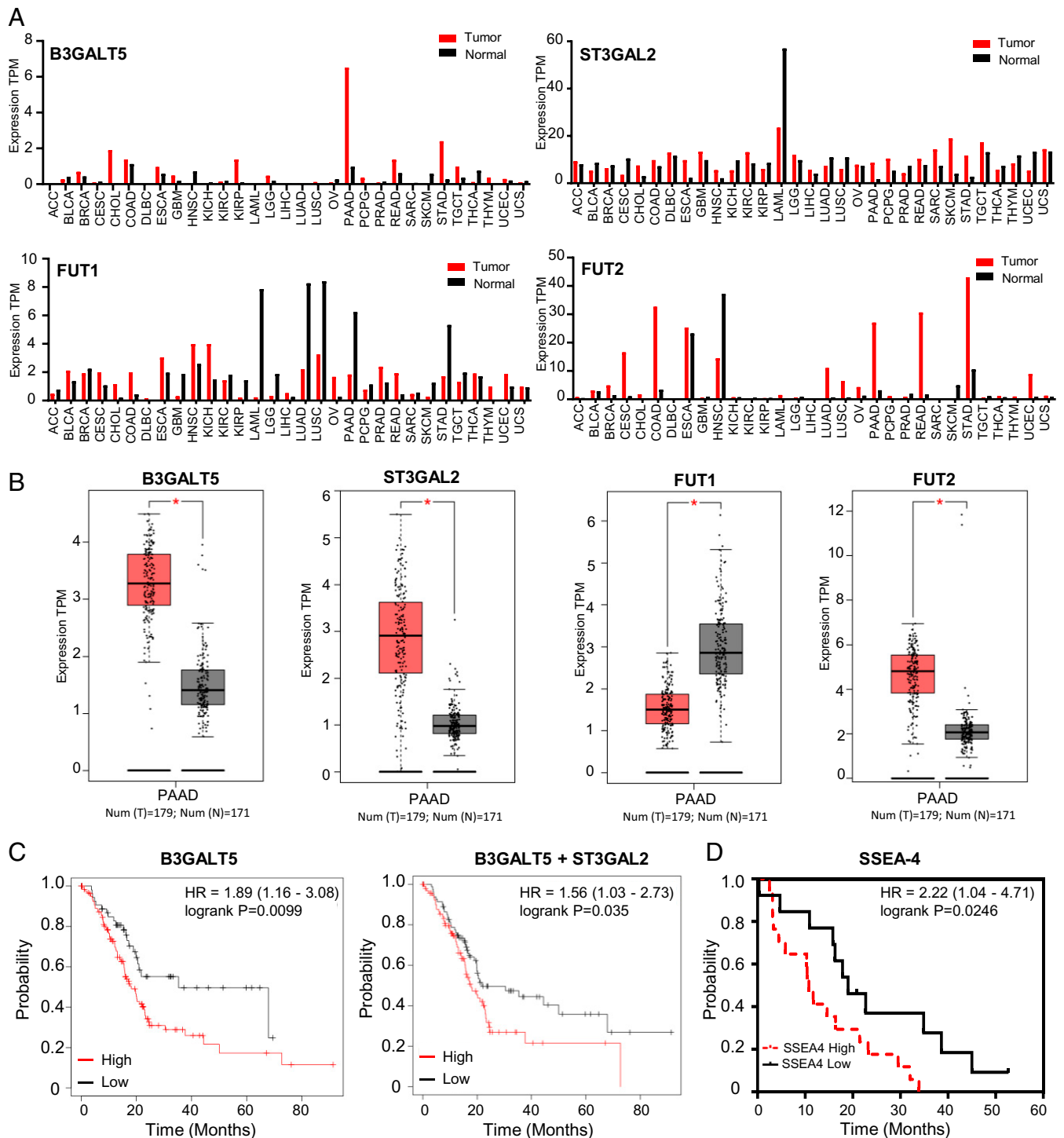


Fig. 2. Survival curves and SSEA-4 expression in pancreatic cancer patients. (A) Expression profiles of *B3GALT5*, *ST3GAL2*, *FUT1*, and *FUT2* across all tumor samples and paired normal tissues. The data were generated in the Gene Expression Profiling Interactive Analysis project (GEPIA). The RNA-seq results are reported as number of transcripts per million (TPM). The height of the bar represents the median expression of a certain tumor type or normal tissue. (B) Expression of *B3GALT5*, *ST3GAL2*, *FUT1*, and *FUT2* in PAAD and normal tissues. Tumor number $n = 179$; normal number $n = 171$. Each dot represents expression of tumor type (red) or normal tissue (black). * $P < 0.05$. (C) Kaplan–Meier plots of overall survival for patients with pancreatic cancer in relation to the expression levels of *B3GALT5* and *B3GALT5 + ST3GAL2*. Hazard ratio (HR), 95% confidence intervals (CI), PADD cancer patients ($n = 177$). The data analysis by KM plotter is described in *SI Appendix, Materials and Methods*. (D) Kaplan–Meier plots of overall survival for patients with pancreatic cancer concerning the expression levels of SSEA-4 antigen. Abbreviations: ACC, adrenocortical carcinoma; BLCA, bladder urothelial carcinoma; BRCA, breast invasive carcinoma; CESC, cervical squamous cell carcinoma and endocervical adenocarcinoma; CHOL, cholangiocarcinoma; COAD, colon adenocarcinoma; DLBC, lymphoid neoplasm diffuse large B cell lymphoma; ESCA, esophageal carcinoma; GBM, glioblastoma multiforme; HNSC, head and neck squamous cell carcinoma; KICH, kidney chromophobe; KIRC, kidney renal clear cell carcinoma; KIRP, kidney renal papillary cell carcinoma; LAML, acute myeloid leukemia; LGG, brain lower grade glioma; LIHC, liver hepatocellular carcinoma; LUAD, lung adenocarcinoma; LUSC, lung squamous cell carcinoma; MESO, mesothelioma; OV, ovarian serous cystadenocarcinoma; PAAD, pancreatic adenocarcinoma; PCPG, pheochromocytoma and paraganglioma; PRAD, prostate adenocarcinoma; READ, rectum adenocarcinoma; SARC, sarcoma; SKCM, skin cutaneous melanoma; STAD, stomach adenocarcinoma; TGCT, testicular germ cell tumors; THCA, thyroid carcinoma; THYM, thymoma; UCEC, uterine corpus endometrial carcinoma; UCS, uterine carcinosarcoma; and UVM, uveal melanoma.

[HR]: 1.89, 95% confidence interval [CI]: 1.16 to 3.08, $P=0.009$), with median survival of 18.17 mo in the high-expression group compared to 35.13 mo in the low-expression group. In addition, high expression of the two enzymes together (*B3GALT5* + *ST3GAL2*) revealed significantly poor OS (HR: 1.56, 95% CI: 1.03 to 2.37, $P=0.035$), with a median survival of 17.73 mo in the high-expression group compared to 21.73 mo in the low-expression group (Fig. 2C); and high expression of the three enzymes together (*B3GALT5* + *FUT1* + *FUT2*) responsible for the synthesis of Globo-H showed poor OS (HR: 1.54, 95% CI: 0.97 to 2.44, $P=0.066$), with a median survival of 19.77 mo in the high-expression group compared to 21.73 mo in the low-expression group (SI Appendix, Fig. S2A), though not as significant as the result from high expression of SSEA-4-associated enzymes.

Because SSEA-4 in cancer cells could be further modified by ST6 *N*-acetylgalactosaminide α -2,6-sialyltransferase 6 (*ST6GALNAC6*) to form sialyl-SSEA-4 or also called disialyl Gb5 (DSGb5) (SI Appendix, Fig. S2B) (25), we wonder whether high expression of *ST6GALNAC6* is associated with OS. However, analysis of clinical data showed that, unlike *ST3GAL2*, high expression of *ST6GALNAC6* did not reduce the survival rate; instead, in certain cases, it increased the survival rate, indicating that expression of *ST6GALNAC6* may down-regulate the progression of pancreatic cancer (SI Appendix, Fig. S2 B and C). It is possible that sialylation of SSEA-4 by *ST6GALNAC6* may actually suppress the role of SSEA-4 in cancer as this enzyme is commonly expressed in normal cells and involved in the biosynthesis of various glycoproteins and glycolipids. We also used tissue staining to investigate the relationship between SSEA-4 expression and the survival rate of pancreatic cancer and found that the median survival for pancreatic cancer patients with low expression of SSEA-4 is 19 mo and 10.78 mo for those with high SSEA-4 expression (Fig. 2D, $*P=0.0246$). These results reveal that increased expression of SSEA-4 or high levels of *B3GALT5* and *ST3GAL2* mRNAs significantly correlates with a lower overall survival rate for patients with pancreatic cancer, indicating that SSEA-4 plays a vital role in the disease and is possibly a promising target for therapeutic development.

Efficacy of SSEA-4 Ab and Homogeneous Glycoform with Improved Effector Functions on Pancreatic Cancer Cells. In an effort to develop potential new treatments for pancreatic cancer, antibodies against SSEA-4 were generated by hybridoma and phage display technology using SSEA-4 conjugate for mice immunization (26). The monoclonal IgG1 antibody MC48 generated in this study and the commercially available mouse IgG3 MC813-70 antibody targeting SSEA-4 were investigated. Both were highly specific for SSEA-4 as shown in the glycan array analysis (SI Appendix, Figs. S3 A–D and S4) and effective in inhibiting the growth of pancreatic tumors in mice (Fig. 3A) at the dosages of 0.5 mg/kg and 1.25 mg/kg, respectively. These two antibodies were then humanized into the chimeric IgG1 glycoforms (hMC48 and chMC813-70) by complementarity determining regions (CDR) grafting for evaluation of human effector functions. The result showed that both chimeric antibodies exhibited excellent cytotoxic activity against pancreatic cancer cells expressing SSEA-4 (SI Appendix, Fig. S5 A–D). To further enhance the effector functions especially Fc γ IIIa-mediated antibody-dependent cellular cytotoxicity (ADCC), we modified the Fc glycans at position Asn-297 to α 2,6-sialyl complex-type biantennary *N*-glycan (SCT) and the corresponding 3F-sialylated derivative (FSCT) as described previously (27) to maximize their interaction with the Fc receptor Fc γ IIIa. We evaluated the antitumor activity of wild-type chMC813-70 and the homogeneous glycoform chMC813-70-SCT as well as the corresponding chMC813-70-FSCT designed to improve the stability and binding with the Fc receptor (Fig. 3 B and C and SI

Appendix, Fig. S6 A–D). The result showed that chMC813-70-SCT and chMC813-70-FSCT are more effective than chMC813-70 against HPAC cells, which have relatively higher SSEA-4 expression than other pancreatic cancer cell lines (Fig. 3C). The half-maximal effective concentrations (EC_{50}) for chMC813-70-FSCT were 5 ng/mL against HPAC, 158 ng/mL against PL-45, and 89 ng/mL against BxPC3, compared to 207 ng/mL, 348 ng/mL, and 159 ng/mL with chMC813-70. Since chMC813-70-SCT has higher avidity toward the Fc γ IIIa receptor ($K_d=0.2$ nM) (27) as compared to the wild-type chMC813-70 (50.5-fold reduction in binding) and the homogeneous antibody chMC813-70-SCT (4.5-fold reduction in binding) to Fc γ IIIa, chMC-813-70-SCT was used to isolate and expand a subpopulation of natural killer (NK) cells enriched with Fc γ IIIa receptor for evaluation of the activity against pancreatic cancer cells (Fig. 3 D and E). The results indeed showed that this subpopulation of NK cells is sixfold more effective than the unseparated NK cells against pancreatic cancer cells based on the killing assay (Fig. 3F). The same result was observed with the use of Fc-SCT only for isolation and expansion as the Fab portion of the homogeneous antibody did not affect the Fc-receptor interaction. Besides, due to cancer heterogeneity, we speculate that pancreatic cancer cells may express SSEA-4, SSEA-3, and Globo-H sequentially or together in a heterogeneous manner, so another antibody, MC607, was generated to target the three globo-series GSL glycans simultaneously (SI Appendix, Fig. S7A). This antibody has complement-dependent cytotoxic (CDC) activity (SI Appendix, Fig. S7B) and strong inhibition of tumor growth in mice at the dosage of 1.25 mg/kg (SI Appendix, Fig. S7C). Taken together, we have demonstrated that chimeric antibodies designed to target SSEA-4 specifically or the three globo-series GSLs simultaneously are effective against pancreatic cancer in vitro and in vivo, and such chimeric antibodies can be converted to homogeneous glycoforms with improved effector functions for treatment of pancreatic cancer and also for isolation of a subpopulation of NK cells with better killing activity against the target cells.

Demonstration of Efficacy in HPAC Tumor-Bearing Mice with Low Numbers of Anti-SSEA-4 CAR-T Cells. To evaluate the potential of cell-based immunotherapy targeting SSEA-4 on pancreatic cancer, we constructed anti-SSEA-4 CAR-T cells using a single-chain variable region (scFv) of an anti-SSEA-4 antibody to assess the safety and killing activity against pancreatic cancer cells in vitro and in vivo. The architecture of CAR constructs used in this study is shown in Fig. 4A, which contains a fragment of anti-SSEA-4 Ab with reverse scFv (VL-linker-VH) incorporated into a CAR plasmid containing the CD28 costimulatory domain and CD3 ζ stimulatory domain. After transduction and activation, CAR-T cells were expanded for 12 d, followed by fluorescence-activated cell sorting (FACS) analysis for CAR expression as monitored by FLAG-tag antibody (Fig. 4B). The cytotoxicity of the HPAC pancreatic cancer cell line was plotted at 4, 24, and 48 h postaddition of CAR-T cells as shown in Fig. 4C. Since the PMC300 CAR-T cells exhibited higher cytotoxicity, the construct PMC300 was selected for further animal study. The pancreatic cancer cell line HPAC was injected into NOD scid gamma (NSG) mice. At the time of tumor formation on day 11, different numbers of anti-SSEA-4 CAR-T cells were injected into mice; one group with phosphate buffered saline (PBS) and the other with 5 million untransduced human T cells as a negative control. As a result, SSEA-4 CAR-T cells demonstrated robust killing activity against pancreatic cancer cells in vitro and pancreatic tumor-bearing mice in vivo with significantly reduced tumor growth rate (Fig. 4 D and E and SI Appendix, Figs. S8 and S9). In addition, we examined the patterns of cytokines including interferon gamma (IFN- γ), interleukin-1beta (IL-1b),

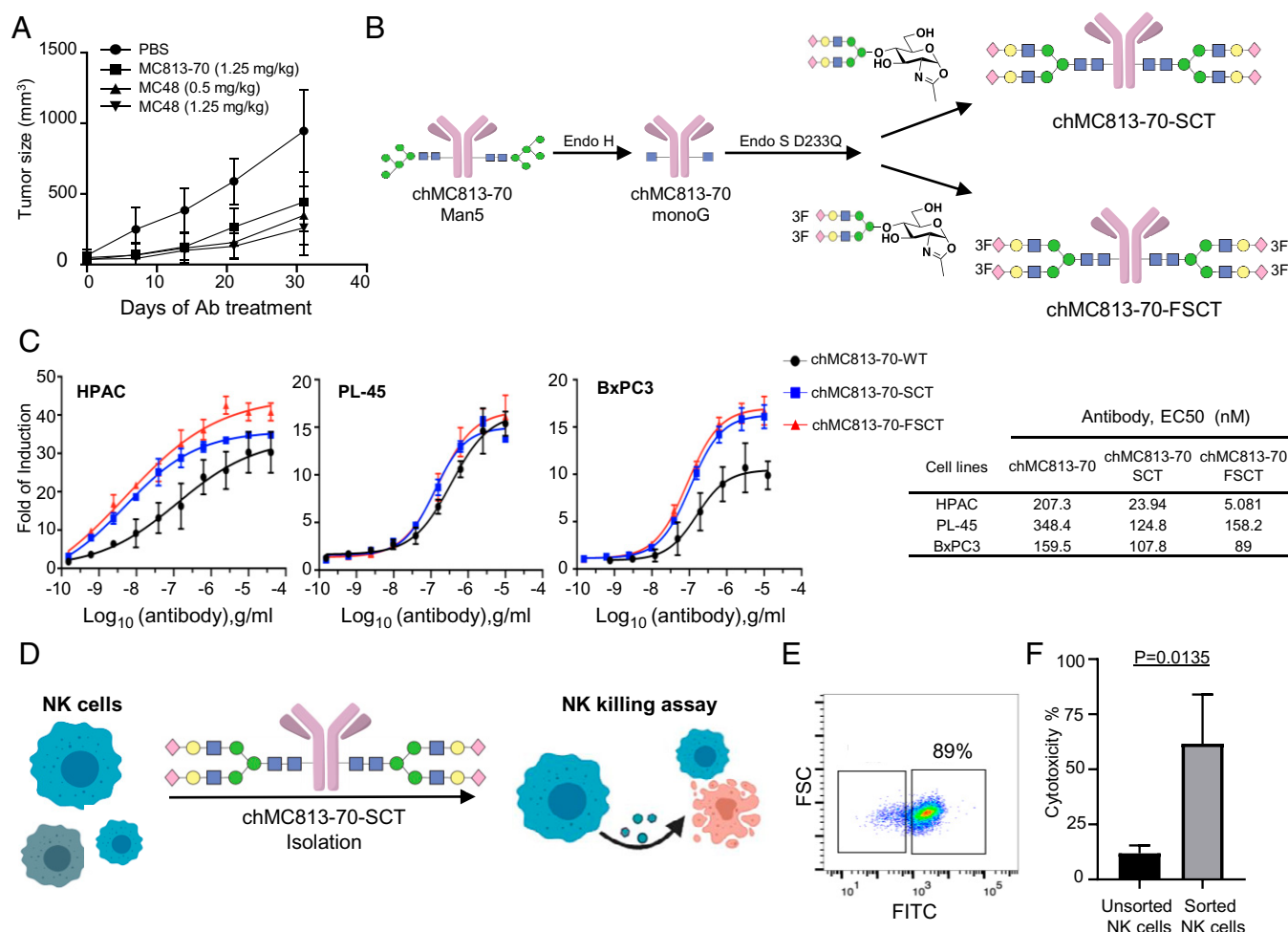


Fig. 3. In vitro and in vivo efficacy of SSEA-4 Ab on pancreatic cancer cells. (A) In the experiments, nude mice were injected with BxPC3 cells (10^6 per mouse). Antibody injection (intraperitoneal [i.p.]) was started when tumors were palpable (40 mm^3) after injecting tumor cells. SSEA-4 Ab (MC48) was administered at a dose of 0.5 mg/kg or 1.25 mg/kg, MC-813-70 was administered at a dose of 1.25 mg/kg, twice per week with i.p. injection until 1 mo. The tumor volume in each group was measured at different time points and shown as mean \pm SD. (B) Scheme of glycoengineering anti-SSEA-4 antibodies to homogeneous antibodies (chMC813-70-SCT and chMC813-70-FSCT) with maximal ADCC activity. (C) ADCC assays of chMC813-70, glycoengineered chMC813-70-SCT, and the corresponding 3-F sialyl derivative (chMC813-70-FSCT) designed to improve stability. Experiments were performed under the effector-to-target (E:T) ratio of 6:1 with target cells (HPAC, PL-45, and BxPC3) and the V158 Fc γ R1IIa-engineered effector Jurkat cells. EC₅₀ is in nanograms per milliliter. (D) Isolation of a subpopulation of primary NK cells by the homogeneous glycoengineered antibody chMC813-70-SCT with maximal ADCC for expansion and killing assay. (E) Flow cytometry of primary NK cells with antibody chMC813-70-SCT (fluorescein isothiocyanate [FITC]-conjugated). (F) Cytotoxicity of expanded human NK cells. The expanded NK cells exhibited stronger cytotoxicity than the primary NK cells against HPAC cells.

interleukin-12p70 (IL-12p70), interleukin-2 (IL-2), interleukin-4 (IL-4), interleukin-6 (IL-6), interleukin-8 (IL-8), interleukin-10 (IL-10), interleukin-13 (IL-13), and tumor necrosis factor alpha (TNF- α) in plasma, and we did not observe significant organ damage in mice. Cytokine profiles (SI Appendix, Fig. S10) were analyzed from mouse plasma on day 24. The most significant mouse cytokines detected include IL-10, IL-12p70, IL-6, and TNF α whereas the most significant human cytokines detected consisted of IFN γ , IL-10, TNF α , and IL-13. The elevation of IL-6 and IL-10 supports the presence of cytokine storms in dying mice. The presence of IFN γ , TNF α , and IL-2 may be consistent with the antitumor activity of anti-SSEA-4 CAR-T cells. The concentration of human IFN- γ , IL-10, TNF α , and IL-13 in mouse plasma correlates with the number of anti-SSEA-4 CAR-T cells injected. In addition, we also analyzed the presence of FLAG, CD3, programmed cell death 1 (PD-1), and T cell immunoglobulin mucin 3 (TIM-3) expression in cells from blood from a terminal bleed (SI Appendix, Fig. S11). PD-1 and TIM-3 are exhaustion markers shown with the frequency of expression in each group.

The high expression of inhibitory receptors Tim-3 and PD-1 will affect the antitumor activity, and they are not highly expressed in our animal studies. FLAG-negative cells (except group 4) overwhelmingly expressed PD-1 and TIM-3 (red) as compared to the FLAG-positive cells. Most FLAG-positive cells were negative for both PD-1 and TIM-1 (double negative [DN]), consistent with the findings of tumor status in the mice. These results demonstrate the efficacy of SSEA-4 CAR-T in mice.

Discussion

PDAC is an aggressive malignant tumor with poor prognosis and limited treatment options. Immune checkpoint therapies, such as PD-1, have no benefit for PDAC. The development of new targeting strategies to treat PDAC is urgently needed. Antibody and CAR-T therapies have been shown to be a promising targeted therapy for treating many cancers, but have rarely been tried in patients with PDAC, mainly due to the lack of appropriate target. In this study, we have shown that all pancreatic cancer cell lines examined in this study have exclusive

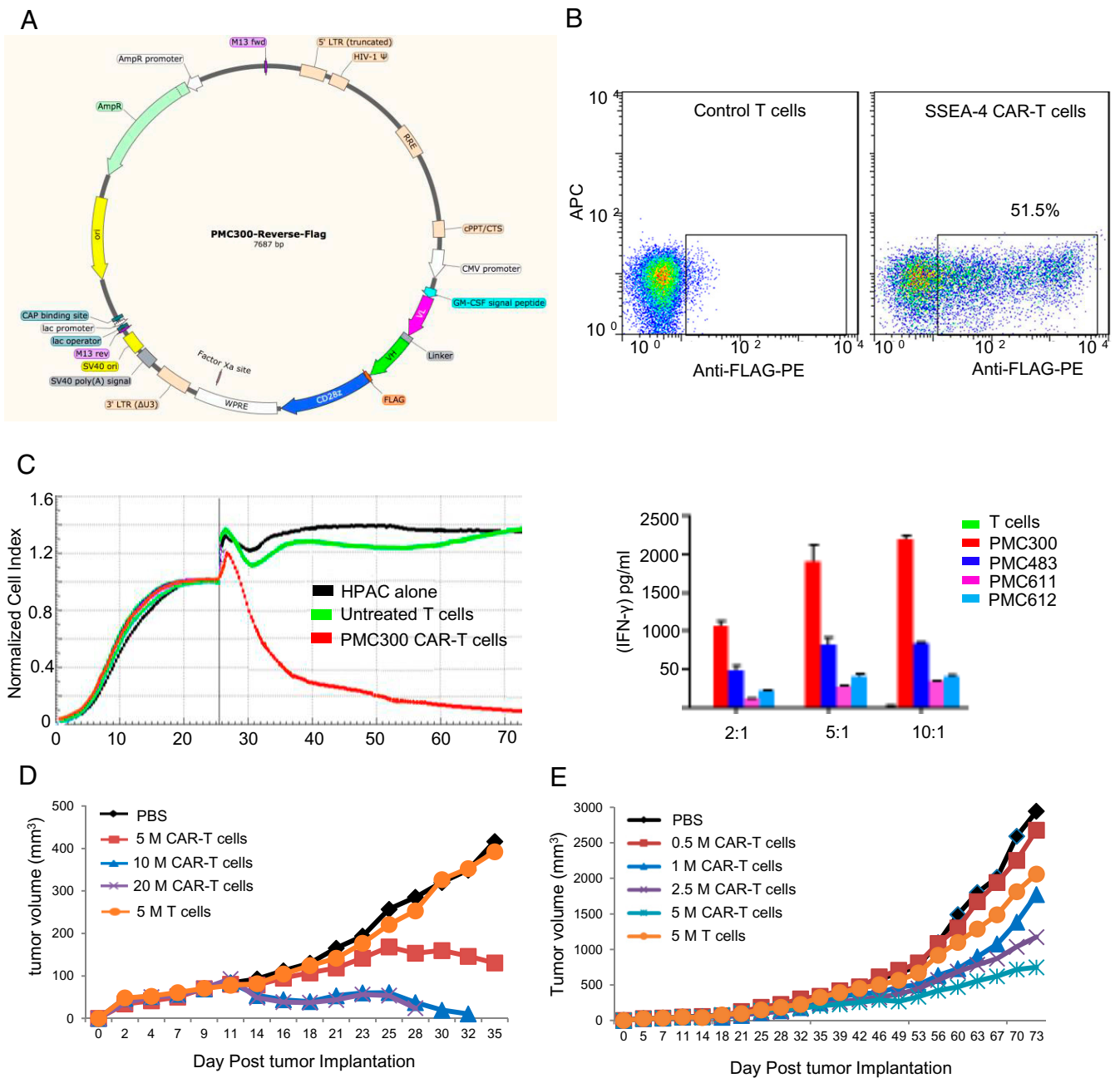


Fig. 4. Anti-SSEA-4 CAR-T cells. (A) An anti-SSEA-4 antibody single-chain variable region (scFv sequence) was subcloned into a lentiviral vector containing CAR cassettes for transduction of human CD4⁺/CD8⁺ T cells. The diagram shows CAR-T constructs. (FLAG = DYKDDDDK). (B) After transduction and activation, CAR-T cells were expanded for 12 d, followed by FACS analysis for CAR expression as monitored by tag antibody. (C) Cytotoxicity of anti-SSEA-4 CAR-T cells against target cells (HPAC) plated onto sample wells to form a monolayer suitable for real-time cytotoxicity assay (RTCA) monitoring. After RTCA measurement, the supernatant from each well was analyzed for human IFN- γ , and among the constructs, PMC300 was selected for further study. (D) Efficacy and toxicity of anti-SSEA-4 CAR-T cells in HPAC tumor-bearing NSG mice. Five million, 10 million, and 20 million CAR-T cells were intravenously injected into NSG mice bearing luminescently tagged HPAC tumors, and a plot of the average tumor volume of each group against treatment time is shown. (E) Sixty NSG mice were implanted subcutaneously with 2 million luminescently tagged HPAC cells and divided into six groups with 10 mice per group. On day 11 when tumors were formed in all mice, 0.5 million, 1 million, 2.5 million, and 5 million anti-SSEA-4 CAR-T cells were injected into four groups of NSG mice; one group with PBS and another group with 5 million untransduced human T cells were used as negative controls. The experiment ended on day 74 and no mouse died or lost body weight.

and high expression of SSEA-4, and pancreatic cancer patients with high expression of SSEA-4, or the enzyme *B3GALT5*, or *B3GALT5* together with *ST3GAL2*, have a poor survival rate. The chimeric anti-SSEA-4 monoclonal antibodies especially their homogeneous glycoforms designed to target SSEA-4 with

optimal effector functions are indeed highly effective against pancreatic cancer in vitro and in vivo, and the NK cells isolated by one of the homogeneous antibodies exhibit enhanced anti-cancer activity as compared to the unseparated NK cells. This is further supported by the construction and demonstration of

anti-SSEA-4 CAR-T cells with reverse scFv construct that are capable of eliminating pancreatic cancer cells in the cell-based and animal studies. In addition, the most commonly observed CAR-T cell-associated toxicity is cytokine release syndrome (CRS). We did not observe the toxicity using our SSEA-4 CAR-T cells. It appears that in addition to the selection of a safe target, the construct of CAR has a major impact on the toxicity and efficacy of CAR-T cell immunotherapy (28–30). In addition, high expression of the inhibitory receptors Tim-3 and PD-1 on tumor-infiltrating lymphocytes affects their antitumor activity, while Tim-3 and PD-1 are not highly expressed in our animal studies. For clinical use, it will require more extensive *in vitro* and *in vivo* testing of SSEA-4 antibody and CAR-T constructs to further verify their safety and efficacy. For example, tissue cross-reactivity testing using various human biological specimens and multiple cytokines should be executed to validate the specificity of the antibody and the safety of SSEA-4 CAR-T cells. Here, the homogeneous antibodies with optimal effector functions and CAR-T cells with reverse scFv designed to target SSEA-4 could become new treatments for PDAC as demonstrated in this proof-of-principle study. Since the specificity of antibody-mediated effector functions is affected by Fc glycosylation, manipulation of antibody Fc-glycan to generate a homogeneous antibody with maximal avidity to specific Fc

receptors could become an effective approach to the study of other effector functions such as FcγIIA-mediated vaccinal effect through dendritic cells (31). In summary, the discovery that high expression of SSEA-4 is associated with poor survival in pancreatic cancer, and the demonstration that targeting SSEA-4 via homogenous antibody or CAR-T strategy can effectively inhibit pancreatic cancer growth in animal models hold significant promise for the treatment of PDAC or other SSEA-4⁺ cancers.

Materials and Methods

See *SI Appendix, Materials and Methods* for a detailed description of cell culture, homogeneous antibody preparation, characterization, humanization and activity assays, and animal models.

Data Availability. All study data are included in the article and/or *SI Appendix*. The data that support the findings of this study are available in Figshare, <https://doi.org/10.6084/m9.figshare.17029595>.

ACKNOWLEDGMENTS. This work was supported by Academia Sinica, through the Summit Program and Ministry of Science and Technology; NIH (AI-130227); and NSF (CHE-1954031). We also thank Profs. P. C. Yang, S. H. Pan, and M. Hsiao for their help in obtaining cell lines; Sachin Shivatare for the glycan drawing; and J. Y. Wang for cellular imaging.

- R. L. Siegel, K. D. Miller, A. Jemal, Cancer statistics, 2019. *CA Cancer J. Clin.* **69**, 7–34 (2019).
- R. E. Royal *et al.*, Phase 2 trial of single agent Ipilimumab (anti-CTLA-4) for locally advanced or metastatic pancreatic adenocarcinoma. *J. Immunother.* **33**, 828–833 (2010).
- R. Winograd *et al.*, Induction of T-cell immunity overcomes complete resistance to PD-1 and CTLA-4 blockade and improves survival in pancreatic carcinoma. *Cancer Immunol. Res.* **3**, 399–411 (2015).
- D. Kabacaoglu, K. J. Ciecieski, D. A. Ruess, H. Algül, Immune checkpoint inhibition for pancreatic ductal adenocarcinoma: Current limitations and future options. *Front. Immunol.* **9**, 1878 (2018).
- N. Vasan, J. Baselga, D. M. Hyman, A view on drug resistance in cancer. *Nature* **575**, 299–309 (2019).
- N. M. Aiello *et al.*, Upholding a role for EMT in pancreatic cancer metastasis. *Nature* **547**, E7–E8 (2017).
- X. Zheng *et al.*, Epithelial-to-mesenchymal transition is dispensable for metastasis but induces chemoresistance in pancreatic cancer. *Nature* **527**, 525–530 (2015).
- A. McGuigan *et al.*, Pancreatic cancer: A review of clinical diagnosis, epidemiology, treatment and outcomes. *World J. Gastroenterol.* **24**, 4846–4861 (2018).
- A. Cid-Arregui, V. Juarez, Perspectives in the treatment of pancreatic adenocarcinoma. *World J. Gastroenterol.* **21**, 9297–9316 (2015).
- J. P. Neoptolemos *et al.*, Therapeutic developments in pancreatic cancer: Current and future perspectives. *Nat. Rev. Gastroenterol. Hepatol.* **15**, 333–348 (2018).
- A. N. Hoseni, R. A. Brekken, A. Maitra, Pancreatic cancer stroma: An update on therapeutic targeting strategies. *Nat. Rev. Gastroenterol. Hepatol.* **17**, 487–505 (2020).
- S. I. Hakomori, The glycosynapse. *Proc. Natl. Acad. Sci. U.S.A.* **99**, 225–232 (2002).
- K. Ohtsubo, J. D. Marth, Glycosylation in cellular mechanisms of health and disease. *Cell* **126**, 855–867 (2006).
- D. H. Dube, C. R. Bertozzi, Glycans in cancer and inflammation—Potential for therapeutics and diagnostics. *Nat. Rev. Drug Discov.* **4**, 477–488 (2005).
- Y. C. Liu *et al.*, Sialylation and fucosylation of epidermal growth factor receptor suppress its dimerization and activation in lung cancer cells. *Proc. Natl. Acad. Sci. U.S.A.* **108**, 11332–11337 (2011).
- M. M. Fuster, J. D. Esko, The sweet and sour of cancer: Glycans as novel therapeutic targets. *Nat. Rev. Cancer* **5**, 526–542 (2005).
- R. D. Astronomo, D. R. Burton, Carbohydrate vaccines: Developing sweet solutions to sticky situations? *Nat. Rev. Drug Discov.* **9**, 308–324 (2010).
- P. O. Livingston *et al.*, Selection of GM2, fucosyl GM1, globo H and polysialic acid as targets on small cell lung cancers for antibody mediated immunotherapy. *Cancer Immunol. Immunother.* **54**, 1018–1025 (2005).
- R. Kannagi *et al.*, Stage-specific embryonic antigens (SSEA-3 and -4) are epitopes of a unique globo-series ganglioside isolated from human teratocarcinoma cells. *EMBO J.* **2**, 2355–2361 (1983).
- M. J. Shablott *et al.*, Derivation of pluripotent stem cells from cultured human primordial germ cells. *Proc. Natl. Acad. Sci. U.S.A.* **95**, 13726–13731 (1998).
- Y. W. Lou *et al.*, Stage-specific embryonic antigen-4 as a potential therapeutic target in glioblastoma multiforme and other cancers. *Proc. Natl. Acad. Sci. U.S.A.* **111**, 2482–2487 (2014).
- P. K. Chuang *et al.*, Signaling pathway of globo-series glycosphingolipids and β1,3-galactosyltransferase V (β3GalT5) in breast cancer. *Proc. Natl. Acad. Sci. U.S.A.* **116**, 3518–3523 (2019).
- Y. J. Liang *et al.*, Switching of the core structures of glycosphingolipids from globo- and lacto- to ganglio-series upon human embryonic stem cell differentiation. *Proc. Natl. Acad. Sci. U.S.A.* **107**, 22564–22569 (2010).
- Y. Kawasaki *et al.*, Ganglioside DSGb5, preferred ligand for Siglec-7, inhibits NK cell cytotoxicity against renal cell carcinoma cells. *Glycobiology* **20**, 1373–1379 (2010).
- S. K. Cheung *et al.*, Stage-specific embryonic antigen-3 (SSEA-3) and β3GalT5 are cancer specific and significant markers for breast cancer stem cells. *Proc. Natl. Acad. Sci. U.S.A.* **113**, 960–965 (2016).
- Y. L. Huang *et al.*, Carbohydrate-based vaccines with a glycolipid adjuvant for breast cancer. *Proc. Natl. Acad. Sci. U.S.A.* **110**, 2517–2522 (2013).
- C. W. Lin *et al.*, A common glycan structure on immunoglobulin G for enhancement of effector functions. *Proc. Natl. Acad. Sci. U.S.A.* **112**, 10611–10616 (2015).
- C. H. June, R. S. O'Connor, O. U. Kawalekar, S. Ghassemi, M. C. Milone, CAR T cell immunotherapy for human cancer. *Science* **359**, 1361–1365 (2018).
- C. Rossig, S. Kailayangiri, S. Jamitzky, B. Altwater, Carbohydrate targets for CAR T cells in solid childhood cancers. *Front. Oncol.* **8**, 513 (2018).
- J. Hartmann, M. Schübler-Lenz, A. Bondanza, C. J. Buchholz, Clinical development of CAR T cells—challenges and opportunities in translating innovative treatment concepts. *EMBO Mol. Med.* **9**, 1183–1197 (2017).
- T. Li *et al.*, Modulating IgG effector function by Fc glycan engineering. *Proc. Natl. Acad. Sci. U.S.A.* **114**, 3485–3490 (2017).